International Journal of Systems Science

ISSN: 0020-7721 (Print) 1464-5319 (Online) Journal homepage: http://www.tandfonline.com/loi/tsys20

A decoupled controller for fuel cell hybrid electric power split

Domenico Di Domenico , Giovanni Fiengo & Anna Stefanopoulou

To cite this article: Domenico Di Domenico , Giovanni Fiengo & Anna Stefanopoulou (2010) A decoupled controller for fuel cell hybrid electric power split, International Journal of Systems Science, 41:4, 447-456, DOI: 10.1080/00207720903072274

To link to this article: http://dx.doi.org/10.1080/00207720903072274

Published online: 16 Mar 2010.

International Journal of Systems Science
Vol. 41, No. 4, April 2010, 447–456

Taylor & Francis
Taylor & Francis Group

A decoupled controller for fuel cell hybrid electric power split

Domenico Di Domenico[a], Giovanni Fiengo[a] and Anna Stefanopoulou[b]*

[a]*Dipartimento di Ingegneria, Università degli Studi del Sannio, Piazza Roma 21, 82100 Benevento, Italy;*
[b]*Mechanical Engineering Department, University of Michigan, Ann Arbor, MI, US*

(*Received 28 September 2007; final version received 12 February 2009*)

The power management of a hybrid system composed of a fuel cell, a battery and a DC/DC power converter is developed. A decoupled control strategy is proposed, aimed at balancing the power flow between the stack and the battery and avoiding electrochemical damage due to low oxygen concentration in the fuel cell cathode. The controller is composed of two components. The first controller regulates the compressor, and as consequence the oxygen supplied to the cathode, via a classic proportional–integral controller. The second controller optimally manages the current demanded by the fuel cell and battery via linear-quadratic control strategy acting on the converter. The closed-loop performance has been tested both in simulation and in real-time simulation using a microprocessor for the controller.

Keywords: fuel cell; hybrid system; power management; optimal control; hardware-in-the-loop

1. Introduction

Fuel cells are considered promising alternative energy conversion systems, thanks to their very high efficiency in converting the chemical energy of hydrogen into electrical energy (Guezennec, Choi, Paganelli and Rizzoni 2003; Vahidi, Stefanopoulou and Peng 2004; Rajashekara 2005) and zero near emissions production (Pukrushpan, Peng and Stefanopuolou 2004; Gao 2005). Apart from the challenges associated with the hydrogen storage and distribution the promise for clean and efficient use of hydrogen still warrants more research and development in fuel cell automation optimisation. One of the key features of the control system devoted to the management of the fuel cell is the supply of oxygen to the cathode (Vahidi et al. 2004; Sun and Kolmanovsky 2005) which is a particularly difficult task during the high-frequency transient in power demand. When current is drawn from a fuel cell, the air supply system should replace the reacted oxygen quickly, otherwise the cathode will suffer from oxygen starvation, which damages the stack and limits the power response. In a high pressure fuel cell, a compressor motor is used to provide the required air into the cathode through a manifold (Vahidi et al. 2004; Pukrushpan, Stefanopoulou and Peng 2005).

To avoid starvation and simultaneously provide the power request, i.e. current demand, it is convenient to add a rechargeable auxiliary power source, which can respond quickly to the increase in current demand.

A battery or a ultracapacitor should be an appropriate auxiliary power source. Both battery and ultracapacitor also appear capable to guarantee good vehicle performance and fuel economy. In this article, we choose a fuel cell hybrid power system (FCHPS) composed of fuel cell and battery.

Furthermore, a DC/DC power converter is placed between them (Figure 1) to optimise the power flow between the fuel cell and the battery and satisfy the load power requirements while ensuring the operation within any limitations of the electrochemical components such as battery over-charge/over-discharge and fuel cell current limit (Jiang, Gao and Dougal 2005).

In the literature, several configurations of hybrid fuel cell systems are proposed (Guezennec et al. 2003; Han, Park, Jeoung, Jeoung and Choi 2003; Nasiri, Rimmalapudi, Emadi, Chmielewski and Al-Hallaj 2004; Vahidi et al. 2004; Holland, Shen and Peng 2005; Jiang et al. 2005). In particular, in Vahidi et al. (2004) a model predictive control of a fuel cell and a small capacitor hybrid system is proposed to avoid oxygen starvation. In Suh and Stefanopoulou (2005) a load following fuel cell system equipped with a compressor and a DC/DC converter is analysed and model-based techniques to tune two separate controllers for the compressor and the converter are shown. In Guezennec et al. (2003), Nasiri et al. (2004) and Jiang et al. (2005) a hybrid system fuel cell-battery is proposed. Different control techniques are illustrated

*Corresponding author. Email: annastef@umich.edu

ISSN 0020–7721 print/ISSN 1464–5319 online

DOI: 10.1080/00207720903072274
http://www.informaworld.com

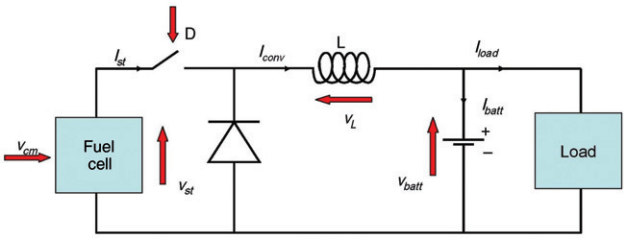

Figure 1. Fuel cell hybrid power system. v_{cm} is the compressor voltage; v_{st} and I_{st} are the voltage and current fuel cell; D is the converter duty cycle; I_{conv} is the converter current; v_L is the inductance voltage; v_{batt} and I_{batt} are the voltage and current battery; I_{load} is the current requested by the load.

depending on the specific aim, i.e. to minimise the hydrogen consumption (Guezennec et al. 2003) or to preserve the battery state of charge and to limit the stack overpotential and voltage drops (Nasiri et al. 2004; Jiang et al. 2005).

In the following, we propose a decoupled control strategy aimed at balancing the power flow between the stack and the battery. In particular, we regulate the input to the motor that drives the fuel cell air flow compressor, and as consequence the oxygen supplied to the cathode, via a classic proportional–integral (PI) controller. We then manage the current demanded to the fuel cell and battery via linear quadratic (LQ) control strategy acting on the converter.

In this article, we first describe the model used for the simulations and the controller design. We then present the adopted control strategy. Software-in-the-loop (SIL) and hardware-in-the-loop (HIL) simulation results and some conclusions end the article.

2. The model

In the following, the models we used to describe and test the proposed control architecture are described. We want to highlight that the fuel cell and the battery models are taken from the recent literature and our contribution is to model how these systems are connected and mainly the adopted control strategy aimed at the power management of the whole system.

2.1. *Fuel cell*

Thanks to its high power density, solid electrolyte, low corrosion and long stack life, the most promising and developed fuel cell technologies for automotive applications is the proton exchange membrane (PEM) fuel cell (Pukrushpan et al. 2004; Stefanopoulou 2004; Rajashekara 2005). In literature several PEM fuel cell models are proposed, each aimed at modelling a particular aspect based on the specific goal. As an example, a static model is proposed in Han et al. (2003) where the fuel cell voltage is described with a static function of the current density. In our work, to include the transient fuel cell behaviour, we used a fuel cell reactant model introduced in Pukrushpan et al. (2004). The dynamic equations are modelled via a non-linear function of the state, the compressor voltage v_{cm} and the fuel cell current I_{st}

$$\dot{x}_{fc} = f_x(x_{fc}, v_{cm}, I_{st}) \tag{1}$$

with the state variables

$$x_{fc} = \left[m_{O_2}\ m_{H_2}\ m_{N_2}\ \omega_{cp}\ \cdots\cdots\ p_{sm}\ m_{sm}\ m_{w,an}\ m_{w,ca}\ p_{rm}\right]^T \tag{2}$$

where m_{O_2}, m_{N_2} and m_{H_2} are respectively the cathode oxygen and nitrogen mass and the anode hydrogen mass; ω_{cp} is the compressor speed; p_{sm} and m_{sm} are the pressure and the inlet air mass in the supply manifold; $m_{w,an}$ and $m_{w,ca}$ are the anode and cathode water mass; p_{rm} is the return manifold pressure. For details on the non-linear equations and the constant parameter values see Pukrushpan et al. (2004, 2005). The model parameters were adjusted to assure a maximum power generation of 75 kW, with a nominal stack voltage of 300 V and a nominal current of 250 A.

Starting from compressor voltage and stack current, the model computes the fuel cell voltage reproducing analytically the air and the hydrogen flows through the fuel cell system components. The compressor, supply manifold, cooler and humidifier are modelled for the air flow path. The hydrogen reaches the stack through its humidifier. The voltage is calculated as a function of stack current, cathode pressure, reactant partial pressures, temperature and membrane humidity. Its open circuit value is calculated from the energy balance between chemical reactant energy and electrical energy, considering the activation, ohmic and concentration losses.

The model outputs are the fuel cell measurements, i.e. stack voltage v_{st} and the compressor air flow rate W_{cp}, and the performance index λ_{O_2}

$$\begin{bmatrix} v_{st} \\ W_{cp} \\ \lambda_{O_2} \end{bmatrix} = f_z(x_{fc}, v_{cm}, I_{st}). \tag{3}$$

At steady state, the compressor air-flow needs to satisfy the reference oxygen excess ratio, $\lambda_{O_2}^{ref}$, based on the following relation:

$$W_{cp}^{ref} = \frac{nM_{O_2}}{4F}\frac{1+\omega_{atm}}{x_{O_2,atm}}\lambda_{O_2}^{ref} I_{st} \tag{4}$$

where n is the number of the stack elementary cells, M_{O_2} the oxygen molar mass, F the Faraday's

constant, ω_{atm} the humidity ratio and $x_{O_2,atm}$ is the oxygen molar fraction in the atmospheric air drawn in the fuel cell.

2.2. *DC DC converter*

The fuel cell and the battery model are coupled via a DC/DC converter which manages the current from the stack and the battery. Typically a DC/DC converter is a device that accepts a DC input voltage and produces a lower or higher DC output voltage.

Here, in the proposed FCHPS, the standard electric configuration of the converter is modified after substituting the capacitor of the DC/DC converter with the battery. The converter inputs are the stack and the battery voltages, v_{st} and v_{batt}, and the outputs are the stack and the battery currents, I_{st} and I_{batt}. The controller acts on the interrupt (Figure 1), regulating the average value of the fraction of time that the converter is conducting, i.e. the interrupt is switched on. This average value is generally indicated as the duty cycle D (Suh and Stefanopoulou 2005), and it is considered as the control input to the system. When the controller drives the interrupt in the state ON, the fuel cell is connected to the load and provides power both to the battery and the load. Conversely, if the interrupt is OFF, the demanded power is provided exclusively by the battery. So, acting on the duty cycle it is possible to determine the average distribution of the power load between the two energy sources balancing the load current on battery and stack.

Now, considering as other inputs to the DC/DC the requested load power P_{load}, the dynamic model can be obtained according to

$$\dot{I}_{conv} = \frac{1}{L}(Dv_{st} - v_{batt}), \tag{5}$$

where the state I_{conv} is the converter current. Finally, the converter outputs are the currents towards the fuel cell and the battery, as follows

$$I_{st} = DI_{conv} \tag{6}$$

$$I_{batt} = I_{conv} - \frac{P_{load}}{v_{batt}}. \tag{7}$$

2.3. *Battery*

Many battery models with different complexity exist in literature. Often a simple model with specific electrical resistor and capacitor to reproduce the electrical properties of the battery connection is used (Gao 2005; Jiang et al. 2005). Sometimes more complex models, i.e. obtained by modelling the kinetic of reactions and the diffusion phenomena (Barbarisi, Glielmo and Vasca 2006) are presented.

In our work, we adopted a simple model (Han et al. 2003). This model describes the variation of the state of charge (SOC) of the battery as a function of the drawn current I_{batt}. In particular, the charge stored or released by the battery is computed simply by integrating the battery current. Hence the input of the model is the current, the state and one of the battery outputs is the SOC, whose derivative is computed by dividing the incoming current by the battery capacity Q_{max}, as follows

$$\dot{SOC} = \frac{I_{batt}}{Q_{max}} \tag{8}$$

where Q_{max} is defined as the maximum electrical charge that the battery can store or equivalently as the maximum current that a battery can deliver for an hour. The outputs are the SOC and the battery voltage v_{batt}, determined by a non-linear experimental static curve function of SOC.

Finally, the hybridisation degree (HD), i.e. the ratio among the nominal power generated by the two sources (Gao 2005)

$$HD = \frac{P_{batt}}{P_{batt} + P_{fc}} \tag{9}$$

is chosen to be equal to 0.5. Hence the battery capacity was chosen equal to 42 Ah.

3. The control strategy

The control objective is to provide the requested power to the load while regulating the battery state of charge and the oxygen ratio of the fuel cell cathode at their nominal values, acting on the converter duty cycle D and the compressor voltage v_{cm}. The problem can be solved with a decoupled control architecture shown in Figure 2. The air flow controller is designed to regulate the oxygen ratio λ_{O_2} feeding back the compressor air flow rate and acting on the compressor voltage. This controller can reach high performance if the stack current is constant or changes slowly. Then, a second controller, working on the converter, optimally regulates the battery state of charge guaranteeing at the same time the requested power (or current to the load) and avoiding the fast transient of the stack current. In particular, it uses the fuel cell to recover the state of charge.

In the following subsections the controllers are described in detail.

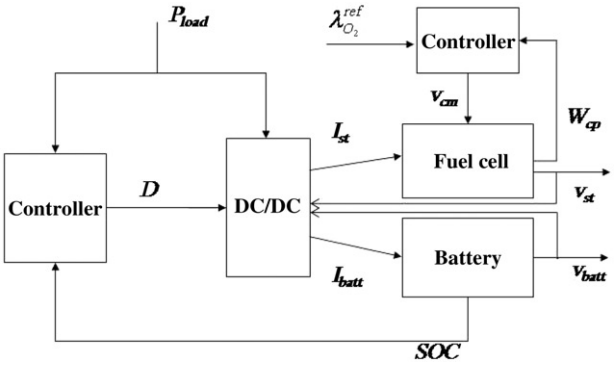

Figure 2. Decoupled control scheme. Some connections are omitted for sake of readability.

3.1. *Fuel cell controller*

One of the key features in fuel cell control is the regulation of the oxygen ratio at the cathode in order to prevent oxygen starvation and, as consequence, the performance and the potential life reduction (Vahidi et al. 2004; Sun and Kolmanovsky 2005). The main problem is that λ_{O_2} is not measurable but it can be regulated at steady state by measuring and regulating W_{cp} to the desired W_{cp}^{ref} that corresponds to a desired $\lambda_{O_2}^{ref}$ as shown in Equation (4). Unfortunately, during the current transients, the error introduced by this approximation propagates to the regulation of the oxygen ratio, causing an inevitable performance reduction. Hence it is critical that the stack current is constant or varies slowly, which can be achieved by opportunely tuning the DC/DC converter controller.

Here, the adopted control strategy is obtained combining a feedback and feedforward action introduced in Stefanopoulou, Pukrushpan and Peng (2004) and Suh and Stefanopoulou (2006), as shown in Figure 3. The first is realised via a PI controller, whose input is the error between the measure of W_{cp} and reference W_{cp}^{ref} for the desired $\lambda_{O_2}^{ref}$. A fixed $\lambda_{O_2}^{ref} = 2$ is considered here, but an optimum $\lambda_{O_2}^{ref}$ can be also utilised as in Arce, Bordons and del Real (2006).

The feedforward controller was found to be an affine function of stack current I_{st}, and this result was confirmed by using the full non-linear simulation

$$v_{cm}^{FF} = 20.16 + 0.712 I_{st}. \tag{10}$$

3.2. *DC/DC controller*

The main component of the proposed architecture is the controller devoted to balance the requested power between the fuel cell and the battery. The objectives are to regulate the state of charge and minimise the rate of variation of the stack current, subject to the constraint

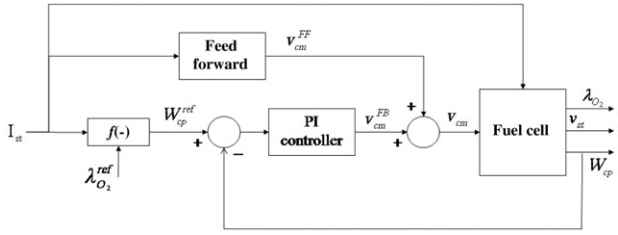

Figure 3. Fuel cell control scheme.

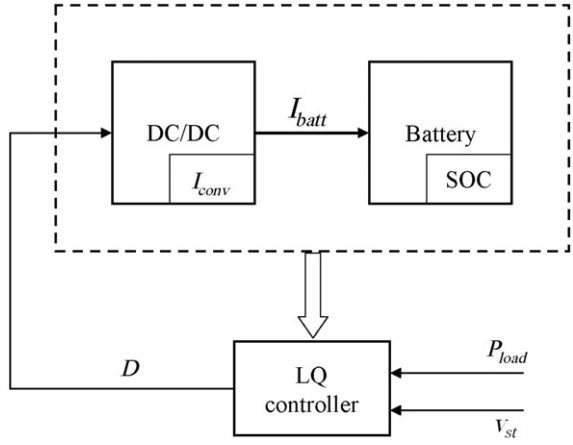

Figure 4. Power management control. Schematic diagram.

on power demand $P_{load} = v_{batt} I_{load}$. The main idea is to have the battery support the load demand and the fuel cell maintain the battery SOC, which varies much slower than the load, hence isolating the fuel cell from high-frequency current demands and variations.

To this aim, due to its simplicity and its intuitive time-domain tuning procedure, the linear quadratic regulation (LQR) technique is used. LQR is designed on the DC/DC converter and battery (Figure 4), whose model Equations (8) and (7) are rewritten as

$$\dot{I}_{conv} = -\frac{1}{L} v_{batt}(SOC) + \frac{1}{L} v_{st}(t) D \tag{11a}$$

$$\dot{SOC} = \frac{I_{conv}}{Q_{max}} - \frac{1}{Q_{max}} \frac{P_{load}(t)}{v_{batt}(SOC)} \tag{11b}$$

where I_{conv} and SOC form the state vector x, D is the control input u, and $v_{st}(t)$ and $P_{load}(t)$ are considered as time varying parameters.

The objective function has been selected after taking into account the goals both on the battery state of charge and on the rate of variation of stack current, as follows

$$V = \frac{1}{2} \int_0^\infty \left[(x - \overline{x})^T Q (x - \overline{x}) + R(u - \overline{u})^2 \right] \mathrm{d}t \tag{12}$$

where $(\overline{x}, \overline{u})$ is the equilibrium point of system (11) related to the desired SOC value, i.e. $\overline{x}_2 = \overline{SOC} = 80\%$, and associated battery voltage $\overline{v}_{batt} = 10.39\,\mathrm{V}$

$$\overline{x}_1 = \overline{I}_{conv} = \frac{P_{load}}{\overline{v}_{batt}} \tag{13a}$$

$$\overline{u} = \overline{D} = \frac{\overline{v}_{batt}}{v_{st}} \tag{13b}$$

with $\overline{x}_1$ and $\overline{v}_{batt}$ the converter current, function of the requested power, and the battery voltage corresponding to $\overline{SOC}$.

We have to highlight that we do not consider a battery state of charge estimator (see as an example, Barbarisi et al. (2006)) but we assume it is known or accurately estimated, since it is out of the scope of the article.

In order to apply the well-known optimal LQ controller, the system (11) is linearized around the equilibrium point (13)

$$\delta\dot{x} = A(t)\delta x + B(t)\delta u \tag{14}$$

where $\delta x = x - \overline{x}$ and $\delta u = u - \overline{u}$ are respectively the deviation of the state and the control input from the desired point, and the time-varying matrices $A(t)$ and $B(t)$ are computed according to

$$A(t) = \begin{pmatrix} 0 & -\dfrac{1}{L}\dfrac{\partial \overline{v}_{batt}}{\partial SOC} \\ \dfrac{1}{Q_{max}} & \dfrac{P_{load}(t)}{Q_{max}\overline{v}_{batt}^2}\dfrac{\partial \overline{v}_{batt}}{\partial SOC} \end{pmatrix} \tag{15a}$$

$$B(t) = \begin{pmatrix} \dfrac{v_{st}(t)}{L} \\ 0 \end{pmatrix} \tag{15b}$$

with $\frac{\partial \overline{v}_{batt}}{\partial SOC}$ the change of battery voltage with respect to the SOC evaluated at the nominal $\overline{SOC}$. Note that linearising the system around the desired SOC value reduces the tracking problem to a regulation to zero problem.

Hence, the objective function (12) is related to the linearised system as follows

$$V = \frac{1}{2}\int_0^\infty \left[\delta x^T Q \delta x + R\delta u^2\right]\mathrm{d}t. \tag{16}$$

The values of the semi-definite positive matrix Q and of the definite positive matrix R were determined using the Matlab/Simulink 'Genetic Algorithm and Direct Search Toolbox', 2005. The quality index was the quadratic error on λ_{O_2} during a step from 30 to 35 kW in requested power and the population size was set to 20. The power split goal allows the management strategy to relax the regulation of the SOC during the most fuel cell stressful manoeuvres, which translates to a larger value for R than Q. The optimal values we found are $Q = \mathrm{diag}(10, 0.143)$ and $R = 10^6$. The control law is

$$\delta u^* = -R^{-1}B(t)^T P \delta x \tag{17}$$

where P is the solution of the Riccati equation. As usual, to avoid an excessive computational cost and to permit an on-line implementation, the suboptimal solution was adopted, obtained by solving the algebraic Riccati equation (Anderson and Moore 1990)

$$P(t)A(t) + A(t)^T P(t) - P(t)B(t)R^{-1}B(t)^T P(t) + Q = 0. \tag{18}$$

The condition for the solution of the Riccati equation existence, i.e. (A, Q) observable and (A, B) controllable, is verified. Finally, the control input can be obtained

$$u^* = \overline{u} - R^{-1}B(t)^T P(x - \overline{x}). \tag{19}$$

4. Simulation results

The performance of the proposed control strategy has been investigated through Matlab/Simulink and real-time simulations. In order to reduce the computational effort during the Matlab/Simulink simulation, the Riccati matrix P was considered constant until the coefficients of the (18), i.e. the matrices A and B, change significantly. These matrices are functions of $P_{load}(t)$ and $v_{st}(t)$, so two dynamic thresholds were set and the values of the Riccati matrix P were updated when the variation of power request or stack voltage was greater then 1%. Conversely, for HIL simulation, a gain scheduling was computed off-line. A grid was determined as a function of the power request and stack voltage. Specifically the range for v_{st} was chosen between $v_{st} = 1$ V and $v_{st} = 400$ V with a step of 1 V (400 values in total). For P_{load} the interval was fixed between $P_{load} = 10$ kW and $P_{load} = 55$ kW with a step of 100 W (450 values in total). The whole grid consisted of 18,000 points. The Riccati equation solution P was computed for each point. In the two following sections the simulation results will be discussed in detail. In particular, the selected results obtained by the HIL simulation show the feasibility and the robustness of the control architecture.

4.1. *SIL simulation*

A large number of simulations was performed to assess the closed-loop performance. A selected

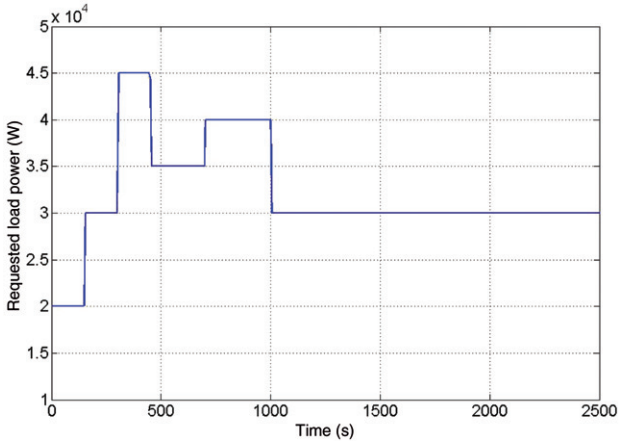

Figure 5. SIL simulation: requested load power.

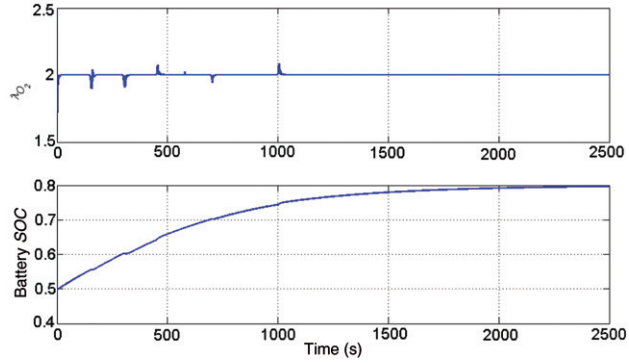

Figure 6. SIL simulation: battery state of charge and oxygen ratio at cathode.

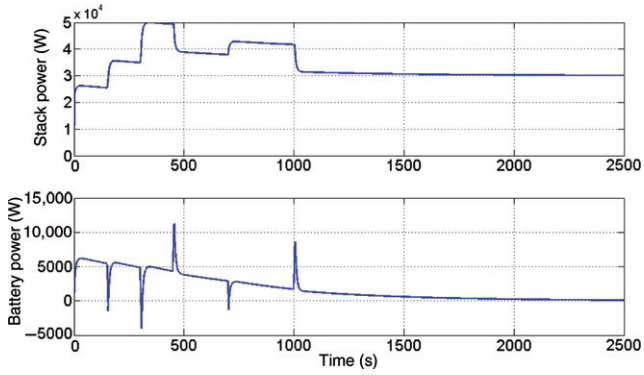

Figure 7. SIL simulation: fuel cell and battery power flow.

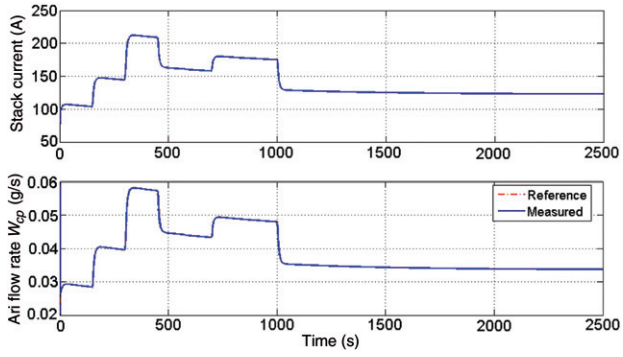

Figure 8. SIL simulation: stack current and compressor air flow rate.

simulation in Matlab/Simulink environment is used to demonstrate the results. Figure 5 shows the selected load profile, which is comprised of steps in power demand. In particular during the first 1000 s the power demand exhibits five steps starting from a minimum value of 20 kW until a maximum value of 45 kW. During the last 1500 s a constant value (30 kW) was set for the power request in order to evaluate the performance of the strategy in recharging the battery from 50% of the total capacity to the desired SOC value ($SOC = 80\%$). Figures 6–9 summarise the simulation results. The first plot of Figure 6 shows that the oxygen ratio reaches accurately the desired value at steady state, and that the error quickly recovers during the fast power transient. The error on λ_{O_2} is mainly due to the approximation error associated with (4) during stack current transients that propagates to the oxygen ratio regulation. This argument is confirmed by the second plot of Figure 8, that shows the performance of the controller aimed at the regulation of the compressor air flow rate. This control difficulty could be mitigated by a λ_{O_2} observer. This is a topic that we are now investigating. Nevertheless we want to highlight that the correct power split filters the stack current, supporting the action of the fuel cell controller in regulating the oxygen ratio. Thanks to this support, a simple PI is sufficient, in the sense of achieving the expected fuel cell control goal.

Figure 7 shows the performance of the power split strategy, namely the regulation of the battery state of charge and the balancing of the power demand between the two sources. Figure 7 also allows the evaluation of the steady-state closed-loop performance, showing that the fuel cell provides both the desired power and, mainly at the beginning, the extra power necessary to charge the battery. Indeed, the second plot of Figure 6 shows that the SOC reaches the desired value. Conversely, during fast

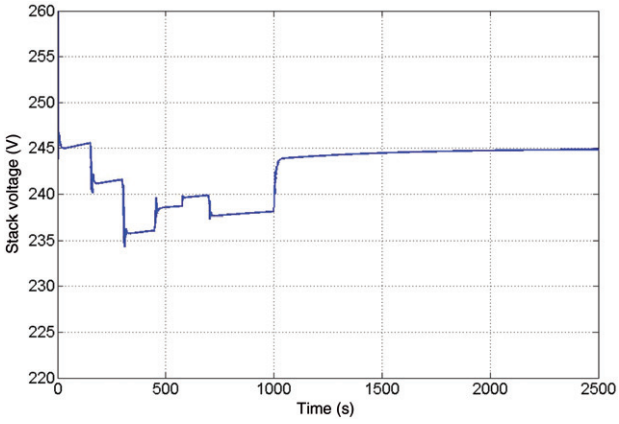

Figure 9. SIL simulation: stack voltage value.

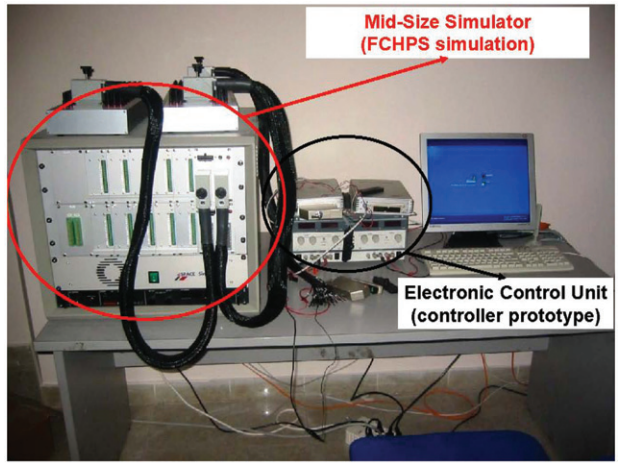

Figure 10. Experimental set-up.

transients, the controller compensates requesting from the battery the amount of power that the fuel cell was not asked to provide in order to maintain high oxygen ratio. The first plot of Figure 8 shows how the controller filters the steps in the power demand allowing a smoother fuel cell current behaviour. Finally, Figure 9 shows the stack voltage. In conclusion, the simulations demonstrate a good behaviour of the controlled system. The controller achieves good balance between the fuel cell and the battery energy supply while providing the power request and reaching the nominal operating point.

4.2. *HIL simulation*

Real-time experiments have been realised connecting a dSpace MicroAutoBox electronic control unit (ECU) with a dSPACE HIL Simulator Mid-Size through a DS2202 I/O board. The MicroAutoBox processor is an IBM PPC 750FX 800 MHz with a total memory of 28 MB, subdivided in main memory, memory for communication with PC and non-volatile flash memory. The processor of the dSPACE HIL Simulator Mid-Size is based on a DS1005 processor board running at 1 GHz and the I/O board has 20 D/A channels and 16 A/D channels, 38 digital inputs and supports two-voltage systems. The dSPACE Simulator reproduced the FCHPS model behaviour while the control strategy was downloaded in the ECU. The experimental set-up is shown in Figure 10. The HIL simulation allows us to test the controller under the ECU prototype feasibility and computational constraints. The closed-loop HIL simulation associated with the load profile shown in Figure 11 is discussed below. Again, the power request values range from 20 and 50 kW. This power demand profile was entered manually on-line during the simulation, except for the step from 35 to 40 kW that was pre-programmed in the ECU. As a consequence, the manual demand steps are not smooth, as the detail in the Figure 11 highlights. Figures 12–14 show the simulation test results. The instantaneous step during the 1000th second demonstrates that the closed-loop performance is consistent with the SIL simulation results. The zoom-in at 1000 s in the first plot of Figure 12 shows that the error on the oxygen ratio is less then 1%. Also the stack current (first plot of Figure 13) and the power split (shown in Figure 14) exhibit the expected behaviour. The battery very quickly supplies the increasing in the power demand allowing the fuel cell current to change slowly. On the other hand, during the manual demanded steps, the oxygen ratio exhibits a larger error, but it is still less than 5%. The increased oscillations are mainly due to the irregularity in the power request profile. The zoom-in at 1500 s in Figures 13 and 14 show that these irregularities also affect the stack current and the battery power behavior. Despite these irregularities, the control strategy achieves its main goal as confirmed by the λ_{O_2} and the SOC regulation.

5. Conclusion

The fuel cell performance can be improved considerably with a hybrid configuration, which combines a battery through a DC/DC converter.

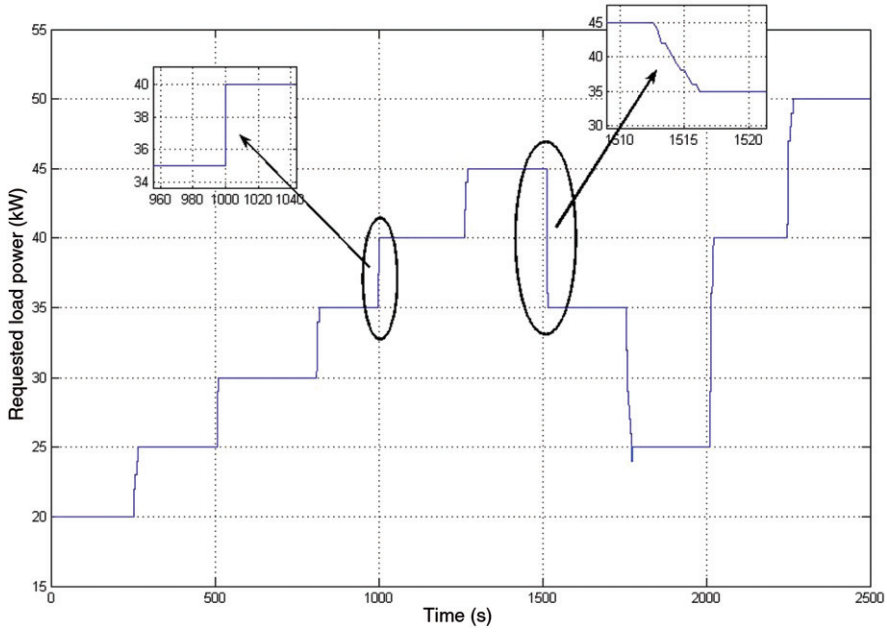

Figure 11. HIL simulation: request load power.

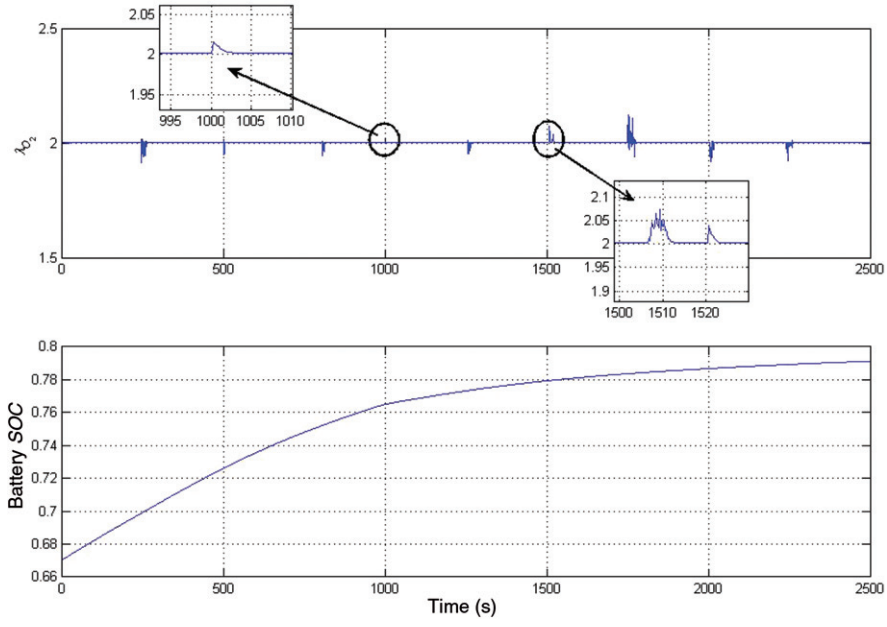

Figure 12. HIL simulation: oxygen ratio at cathode and battery state of charge.

This article shows a simple decoupled control strategy, which allows a good compromise between high performance and safe use of the stack. Here, the fuel cell stack is controlled via a feedforward action and a PI regulator, whereas the DC/DC converter optimises the current split via a linear quadratic controller.

Good closed-loop performance is shown in the HIL experiments. In future work we intend to extend this control strategy after taking into account more realistic constraints in the battery power response, by including *SOC* estimation and inserting in the control loop an observer for the oxygen ratio at the fuel cell cathode.

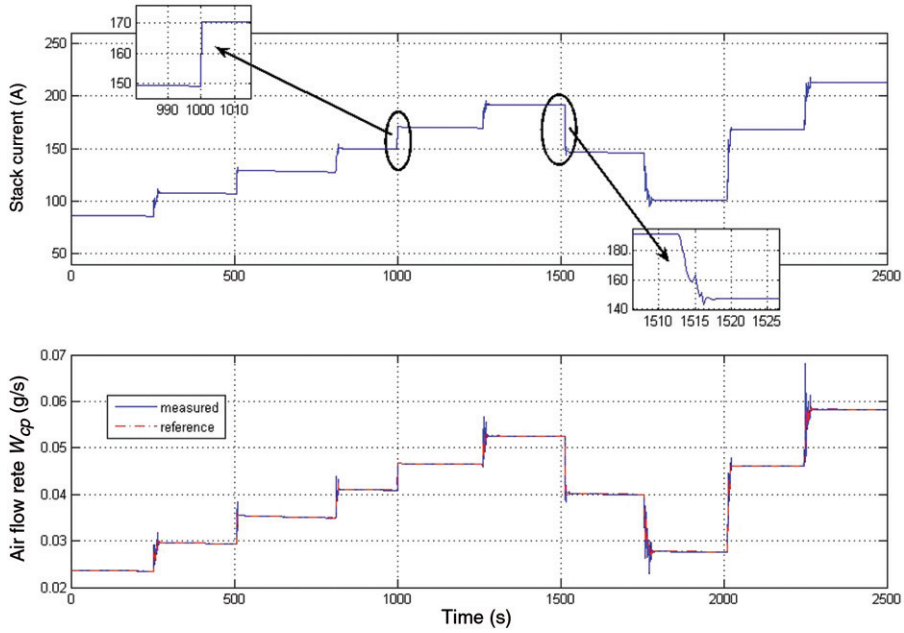

Figure 13. HIL simulation: stack current and compressor air flow rate.

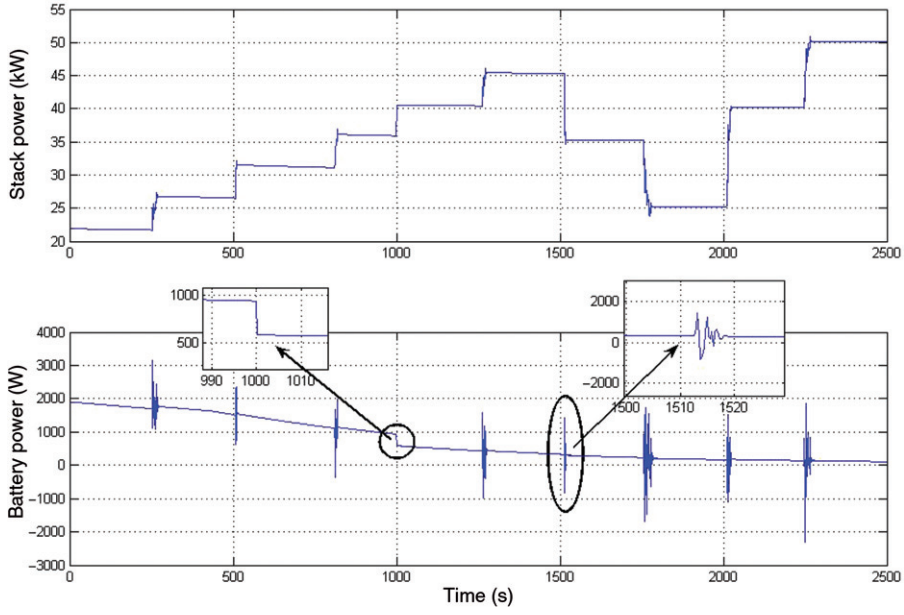

Figure 14. HIL simulation: fuel cell and battery power flow.

Notes on contributors

Domenico Di Domenico obtained his laurea degree cum laude in Physics at the Università di Napoli Federico II in 2002. He obtained his Masters in control of hybrid vehicles in 2005 and his PhD degree in 'Ingegneria dell' 'Informazione' at the Università del Sannio in 2008. He went several times abroad to study, in particular at the University of Michigan in Ann Arbor (USA). Presently he is PostDoc at IFP in Lyon, France. His main research interest lies in the development and the application of innovative methodologies in the fuel cell electric hybrid vehicles modelling and control field. His research topics in this field were the optimal management of the power flow and the battery state of charge estimation. His other research topic is the vehicle localisation. He has collaborated with several research laboratories (Centro Ricerche FIAT in Torino; University of Michigan in Ann Arbor, USA; ELASIS in Napoli) and has participated in several research projects. He is also the author of international scientific publications.

Giovanni Fiengo obtained his laurea degree cum laude in Computer Science Engineering at the Università di Napoli Federico II, in 1998, with a thesis on 'Modelling and identification of the internal combustion engine and catalytic converter for control applications'. The thesis has been developed in collaboration with Magneti Marelli, Bologna, Italy. He obtained his PhD degree in 'Ingegneria dell'Informazione' at the Università di Napoli Federico II, in 2001, with a thesis on 'Modelling, Control and Diagnosis of the Three-Way Catalytic Converter and the Internal Combustion Engine'. He actively collaborates with several universities and research centres. In particular, he collaborates with Ford Research Laboratory in Dearborn (MI, USA), University of Michigan in Ann Arbor (MI, USA), Istitut Francais du Petrol in Lione (France) and, recently, with The Duke University in Durham (NC, USA). Since 1 November 2002 he is an assistant professor at Engineering Department of Università del Sannio in Benevento. His main research activity deals with the modelling and control of spark ignition internal combustion engines, the three-way catalytic converters, battery modelling and hybrid vehicles. Recently, he developed interest in bioengineering field, with particular interest in the deep brain stimulation.

Anna G. Stefanopoulou obtained her Diploma (1991, Nat. Tech. Univ. of Athens, Greece) in Naval Architecture and Marine Engineering and her PhD (1996, University of Michigan) in Electrical Engineering and Computer Science. She is a professor of mechanical engineering at the University of Michigan. She was an assistant professor (1998–2000) at the University of California, Santa Barbara and a technical specialist (1996–1997) at Ford Motor Company. She is a Fellow of the American Society of Mechanical Engineers, and a Fellow of the Institute of Electrical and Electronics Engineers. She has a book on Control of Fuel Cell Power Systems, nine US patents and numerous publications. Her current work addresses the control and automation issues associated with fuel cells, fuel processing and internal combustion engines.

References

Anderson, B.D.O., and Moore, J.B. (1990), *Optimal Control: Linear Quadratic Methods*, New Jersey: Prentice Hall.

Arce, A., Bordons, C., and del Real, A.J. (2006), 'Constrained Predictive Control Strategies for PEM Fuel Cells', in *Proceedings of the 2006 American Control Conference*, Minneapolis, Minnesota, USA, June 14–16.

Barbarisi, O., Glielmo, L., and Vasca, F. (2006), 'State of Charge Kalman Filter Estimator for Automotive Batteries', *Control Engineering Practice*, 14, 267–275.

Gao, W. (2005), 'Performance Comparison of a Fuel Cell-Battery Hybrid Powertrain and a Fuel Cell-Ultracapacitor Hybrid Powertrain', *IEEE Transactions on Vehicular Technology*, 54, 846–855.

Genetic Algorithm and Direct Search Toolbox 2 – Users Guide. Mathworks, 2005.

Guezennec, Y., Choi, T.-Y., Paganelli, G., and Rizzoni, G. (2003), 'Supervisory Control of Fuel Cell Vehicles and its Link to Overall System Efficiency and Low-level Control Requirements', in *American Control Conference*, pp. 2055–2061.

Han, S.-B., Park, S.-I., Jeoung, H.-G., Jeoung, B.-M., and Choi, S.-W. (2003), 'Fuel Cell-Battery System Modeling and System Interface Construction', in *The 29th Annual Conference of the IEEE Industrial Electronics Society*, Vol. 3, pp. 2623–2627.

Holland, K., Shen, M., and Peng, F.Z. (2005), 'Z-Source Inverter Control for Traction Drive of Fuel Cell-battery Hybrid Vehicles', in *Industry Applications Conference*, IAS Annual Meeting, Vol. 3, pp. 1651–1656.

Jiang, Z., Gao, L., and Dougal, R.A. (2005), 'Flexible Multiobjective Control of Power Converter in Active Hybrid Fuel Cell/battery Power Sources', *IEEE Transactions on Power Electronics*, 20, 244–253.

Nasiri, A., Rimmalapudi, V.S., Emadi, A., Chmielewski, D.J. and Al-Hallaj, S. (2004), 'Active Control of a Hybrid Fuel Cell-battery System', in *The 4th International Power Electronics and Motion Control Conference*, Vol. 2, pp. 491–496.

Pukrushpan, J.T., Peng, H., and Stefanopuolou, A.G. (2004), 'Control-Oriented Modeling and Analysis for Automotive Fuel Cell System', *ASME Journal of Dynamic Systems, Measurement, and Control*, 126, 14–25.

Pukrushpan, J.T., Stefanopoulou, A.G., and Peng, H. (2005), *Control of Fuel Cell Power Systems: Principles, Modeling, Analysis and Feedback Design*, London: Springer.

Rajashekara, K. (2005), 'Hybrid Fuel-Cell Strategies for Clean Power Generation', *IEEE Transactions on Industry Applications*, 41, 682–689.

Stefanopoulou, A.G. (2004), 'Mechatronics in Fuel Cell Systems', in *Proceedings of the International Federation of Control, Symposium in Mechatronics*, Sydney, September.

Stefanopoulou, A.G., Pukrushpan, J.T., and Peng, H. (2004), 'Controlling Fuel Cell Breathing.', *IEEE Control Systems Magazine*, 24, 30–46.

Suh, K.-W., and Stefanopoulou, A.G. (2005), 'Control and Coordination of Air Compressor and Voltage Converter in Load-following Fuel Cell.', *International Journal of Energy Research*, 29, 1167–1189.

Suh, K.-W., and Stefanopoulou, A.G. (2006), 'Effects of Control Strategy and Calibration on Hybridization Level and Fuel Economy in Fuel Cell Hybrid Electric Vehicle', in *SAE Paper 06P-428*.

Sun, J., and Kolmanovsky, I.V. (2005), 'Load Governor for Fuel Cell Oxygen Starvation Protection: A Robust Nonlinear Reference Governor Approach', *IEEE Transactions on Control Systems Technology*, 13, 911–920.

Vahidi, A., Stefanopoulou, A.G., and Peng, H. (2004), 'Current Management in a Hybrid Fuel Cell Power System: A Model Predictive Control Approach', *IEEE Transactions Control System Technology*, 14, 1047–1057.